



HAL
open science

Al-Pt MOCVD coatings for the protection of Ti6242 alloy against oxidation at elevated temperature

Mathieu Delmas, Dominique Poquillon, Yolande Kihn, Constantin Vahlas

► **To cite this version:**

Mathieu Delmas, Dominique Poquillon, Yolande Kihn, Constantin Vahlas. Al-Pt MOCVD coatings for the protection of Ti6242 alloy against oxidation at elevated temperature. *Surface and Coatings Technology*, 2005, 200 (5-6), pp.1413-1417. 10.1016/j.surfcoat.2005.08.028 . hal-03601144

HAL Id: hal-03601144

<https://hal.science/hal-03601144>

Submitted on 8 Mar 2022

HAL is a multi-disciplinary open access archive for the deposit and dissemination of scientific research documents, whether they are published or not. The documents may come from teaching and research institutions in France or abroad, or from public or private research centers.

L'archive ouverte pluridisciplinaire **HAL**, est destinée au dépôt et à la diffusion de documents scientifiques de niveau recherche, publiés ou non, émanant des établissements d'enseignement et de recherche français ou étrangers, des laboratoires publics ou privés.

Al–Pt MOCVD coatings for the protection of Ti6242 alloy against oxidation at elevated temperature

Mathieu Delmas^a, Dominique Poquillon^a, Yolande Kihn^b, Constantin Vahlas^{a,*}

^a Centre Interuniversitaire de Recherche et d'Ingénierie des Matériaux (CIRIMAT-CNRS) ENSIACET, 118 Route de Narbonne, 31077 Toulouse cedex 4, France

^b Centre d'Elaboration de Matériaux et d'Etudes Structurales (CEMES-CNRS), 29 rue Jeanne Marvig, 31055 Toulouse, France

Abstract

Results on isothermal oxidation at 873 K for 90 h of Al–Pt coatings on Ti6242 coupons are reported. These coatings were obtained by low temperature, low pressure metalorganic chemical vapor deposition using $\text{Me}_3(\text{MeCp})\text{Pt}(\text{VI})$ and dimethylethylamine alane. Three coating architectures were investigated, namely pure Al, Pt and Al sequential sublayers, and co-deposited Al and Pt. Oxidation kinetics revealed a strong transient oxidation regime followed by a diffusion driven parabolic one. Such coatings allow to decrease oxidation kinetics more than one order of magnitude compared with those of the bare Ti6242. Scanning electron microscopy, second ion mass spectrometry, X-ray diffraction and transmission electron microscopy revealed that these coatings present a rough surface morphology. They are dense, they develop scales composed of $\gamma\text{-Al}_2\text{O}_3$ and $\delta\text{-Al}_2\text{O}_3$ and they prevent titanium diffusion from the alloy to the surface.

It is concluded that coatings produced by this process show promise for use as effective protection against oxidation of Ti6242 alloys and consequently they may raise the maximum operating temperature tolerated by corresponding parts in helicopter turboengines.

Keywords: Organometallic CVD; Aluminium; Platinum; Titanium alloy; Isothermal oxidation

1. Introduction

Due to their good creep properties, titanium alloys such as Ti6242 could be used for manufacturing of helicopter turbine components submitted to moderate stresses. Expected temperatures to be met by these components are below 723 K and oxidation can be neglected. However, turbines can experience short events at higher temperature during incidental operations. Such events, considered as short oxidation at temperature as high as 823 K, must be taken into account for turbine components. Consequently, coatings which are able to sustain cyclic oxidation and to reduce or prevent the oxidation of titanium alloys up to 823 K would be very attractive.

In analogy with solutions adopted for superalloys, the application of alumina forming coatings such as those containing aluminum and platinum is a potential solution for

the extension of the use of titanium alloys at higher temperature, and consequently at hotter parts of the turbine. However, state of the art processes for the preparation of such coatings (such as electroplating 5–10 μm of Pt followed by heat treatment and aluminization by pack cementation) are complex and involve pollution hazards [1]. More importantly, pack cementation and the required diffusion treatment need the alloy to be heated at high temperatures for several hours. Such treatment will modify the microstructure and consequently the properties of the above mentioned titanium alloys and therefore is prohibited. An alternative, low temperature (typically less than 773 K) and if possible simpler process is necessary in the present case for the deposition of the alumina forming coating.

To face this problem, we recently proposed the application of an Al–Pt coating on Ti6242 coupons using a sequential two step metalorganic chemical vapor deposition (MOCVD) process employing trimethyl-methylcyclopentadieny platinum (IV) $\text{Me}_3(\text{MeCp})\text{Pt}(\text{IV})$ and tri-isobutylaluminum (TIBA) [2]. Although processing conditions were compatible with constraints imposed by the substrate, the

main concern with this work was the discontinuous morphology of Al, deposited on the surface of the inner layer of Pt.

The present work reports on the behavior in isothermal oxidation of coatings that have been produced by improving the above process. Improvements concern (i) the replacement of TIBA by dimethylethylamine alane (DMEAA) and (ii) the co-deposition of Al and Pt. The behavior of the uncoated materials and of the most promising of the coatings processed from TIBA is also reported for comparison. DMEAA, a well known precursor for the deposition of Al films for microelectronics, was selected for its higher growth rate and lower deposition temperature than TIBA [3,4]. Co-deposition of Al and Pt is expected to approach the microstructure of platinum aluminide coatings deposited by high temperature state of the art processes and therefore to meet easier and more efficiently the requirements on the protection of the substrate against high temperature oxidation.

In that which follows, experimental conditions on both processing and oxidation of the coatings will be introduced first. Then, isothermal oxidation of three coating architectures will be presented and discussed in terms of transient and steady state oxidation kinetics obtained from thermogravimetric analysis. These architectures are (i) pure Al taken as reference, (ii) two sub layers, the inner of Pt and the outer of Al and, (iii) co-deposited Al and Pt. Finally, oxidation kinetics will be related to the microstructure of both the coatings and the alumina scale. Due to the limited length of this contribution, microstructural characterization will be limited to the most promising coating configuration. A detailed and systematic characterization of the as deposited and oxidized coatings will be presented in forthcoming papers.

2. Experimental

Depositions were performed in a vertical, cold wall CVD reactor, designed to coat in one run all sides of a 2 mm thick, 15 mm diameter Ti6242 disk for subsequent high temperature oxidizing treatments. Details on this experimental setup are reported in [2]. Adduct grade DMEAA (Epichem) and 99% Me₃(MeCp)Pt(VI) (Strem) were used as received.

Deposition of Al and Pt from these two precursors can be performed in temperature ranges 423 K–523 K and 393 K–623 K, respectively, so that their codeposition is possible. Table 1 reviews the deposition conditions for the different coatings, namely RefAl, Seq1, Cod1 and Cod2. H₂ flow was added in the input gas to decrease the growth rate of Al and to achieve smoother morphology of the coating. Continuous, dense Al coatings were obtained by adding to the input gas a continuous flow of ethyl iodide (C₂H₅I) vapors which acted as a surfactant.

Isothermal oxidation tests were conducted in a SETARAM TAG24S equipment at 873 K during 90 h. This apparatus combines the advantages of good accuracy (better than 1 μg) and reduced buoyancy effects counterbalanced by using a symmetrical furnace with an inert sample. Oxidation was carried out in atmospheric pressure flowing synthetic air with heating and cooling rates of 1°/s. The mass variations are automatically recorded.

Samples were characterized by scanning electron microscopy (SEM) with a LEO 435 VP apparatus equipped with an X-ray energy dispersive spectroscopy (EDS) analyzer, by X-ray diffraction (XRD) in grazing incidence (omega=2°) with a Seifert 3000 TT apparatus and by secondary ion mass spectrometry (SIMS) with a CAMECA IMS4F6 apparatus. In addition, transmission electronic microscopy (TEM) was performed using a Phillips CM20 instrument at electron beam energy of 200 keV, coupled with EDX and electron energy loss spectrometry (EELS) analyzers. Cross sections were prepared by mounting face to face with resin, clamped and heating together two coupons of each sample. The obtained piece was diamond-sawed to slices approximately 300 μm thick, followed by mechanical polishing and finally by ion milling during 2 to 3 h using a Gatan Precision Ion Polishing System (PIPS) equipment until a hole was detected. The PIPS was operated at an acceleration voltage of the ion gun of 5 keV, a rotation frequency of 6 rpm, and an incidence angle of the two ion beams on both sides of the sample of 7°.

3. Results and discussion

Fig. 1 presents the net mass gain (Δm) per unit area (mg cm⁻²) of sample Seq1 as a function of the time maintained

Table 1
Processing conditions for the deposition of the (Al–Pt) coatings

Code	Pt deposition							Al deposition						
	$Q_{N_2,dil}$	$Q_{N_2,Pt}$	Q_{H_2}	Q_{Pt}	t	T	P	$Q_{N_2,dil}$	$Q_{N_2,Al}$	Q_{H_2}	Q_{Al}	t	T	P
RefAl	–	–	–	–	–	–	–	40.5	1.8	12	0.0443	120	523	1.33
Seq1	225	9	75	0.0242	30	473	9.33	41	2.82	0	0.0241	60	473	1.33
Cod1	225	14.4	54	0.0388	120	523	9.33	225	3.2	54	0.0433	120	523	9.33
Cod2	40.5	9	12	0.1697	120	523	1.33	40.5	1.8	12	0.1088	120	523	1.33

$Q_{N_2,dil}$ and Q_{H_2} are flow rates of dilution N₂ and of H₂. $Q_{N_2,Pt}$ and $Q_{N_2,Al}$ are flow rates of N₂ through (MeCp)Me₃Pt (maintained at 327 K) and through DMEAA (maintained at 273 K) bubblers, respectively. Q_{Pt} and Q_{Al} are estimated flow rates of the two precursors. Flow rates are in standard cubic centimeters per minute (sccm). t , T and P are deposition time (min), temperature (K) and pressure (kPa), respectively.

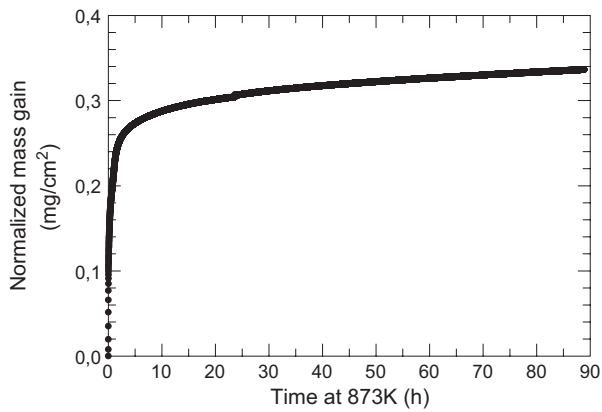


Fig. 1. Mass gain per unit area versus time during oxidation at 873 K of sample Cod2.

at 873 K. After an initial transient oxidation rate, the mass-gain curve is parabolic as expected for diffusion-driven oxidation phenomena. This behavior was confirmed by plotting Δm versus square root of time. When the alumina scale is formed at the coating surface, oxidation is expected to take place by diffusion of species through oxide scale. Scale growth kinetics was interpreted by using the most general expression for parabolic kinetics:

$$t = a + b\Delta m + c\Delta m^2 \quad (1)$$

where t is the time (s). Coefficient c is equal to the reciprocal of the parabolic rate constant k_p ($\text{mg}^2 \text{cm}^{-4} \text{s}^{-1}$) and independent of the initial conditions for integration of the rate equation. Eq. (1) was fitted to a parabola branch, in the range (70 h–90 h) of the $(t, \Delta m)$ data to get the steady state value of k_p [5].

The histogram of Fig. 2 presents the steady state values of k_p for uncoated bare Ti and Ti6242 and for the coated coupons. It should be noticed that all coatings provide improved oxidation resistance relatively to uncoated samples. However, improvement due to Seq0; i.e. sequential sample processed by using TiBA [2] is insufficient, k_p being even higher than that of RefAl. k_p values of RefAl and Cod1 samples do not show any significant difference. This would suggest that the presence of Pt in the coatings does not

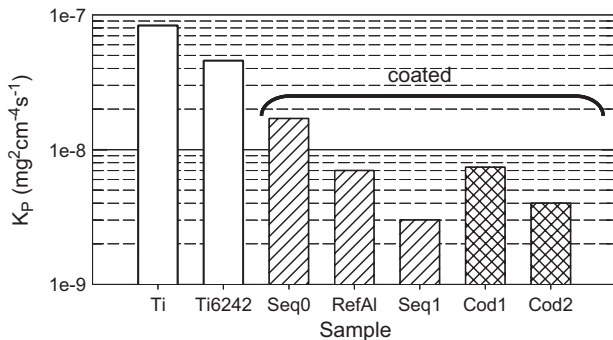


Fig. 2. Parabolic rate constants for the oxidation of pure Ti, of uncoated Ti6242, of a Al–Pt sequential coating processed from TiBA [2], and of the coated samples investigated in the present study.

improve directly the isothermal oxidation resistance but, in agreement with literature reports, it is expected to act more as a cyclic oxidation improving element [6,7]. Coatings Seq1 and Cod 2 present the lowest k_p values, 3×10^{-9} and 4×10^{-9} respectively. These values are more than one order of magnitude lower than that of bare Ti6242.

Fig. 3 presents two SEM micrographs of the surface of sample Cod2, as processed (a) and oxidized (b). The morphology observed in micrograph (a) is relatively rough, porous and granular. The coating grain size is about 350 nm. This morphology is maintained after oxidation (b) with however the following noticeable modifications: (i) the grains size is increased to approximately 1 μm , (ii) the grains shape is now faceted and (iii) the open porosity seems more developed than before oxidation. SEM observations on cross sections of this sample revealed that the observed morphology concerns only the upper layers of the Al coating; the core of the coating is compact and is strongly adherent to the substrate through an extended interdiffusion layer whose thickness is between 30 μm and 50 μm . This layer is mainly composed of Al_3Ti as was shown by XRD but it possibly contains traces of other titanium aluminides. At the boundary between the interdiffusion zone and the coating, Pt-containing nanoparticles are found. EELS revealed that they are formed of a Pt-rich core also containing a small quantity of Al and of an outer layer which contains both Pt and Al. Pt was not found elsewhere in the coating while platinum aluminide Al_2Pt was identified by XRD. It is thus concluded that the latter compound is

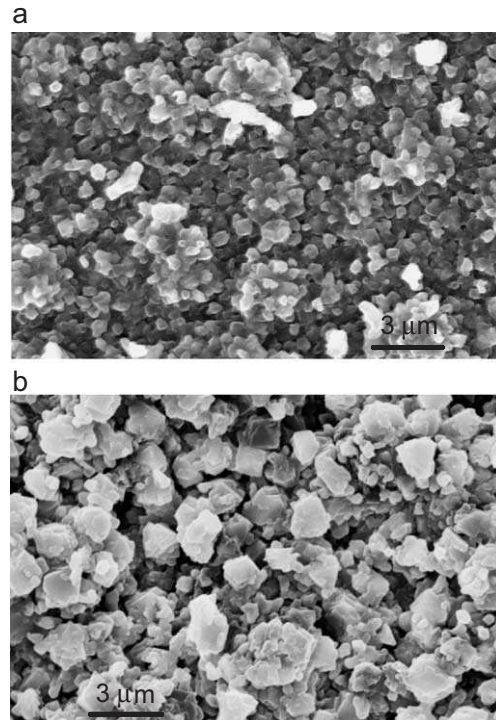


Fig. 3. SEM micrographs of the surface of the Cod2 sample, as deposited (a) and after oxidation (b).

formed during oxidation from the incomplete interdiffusion between the Al coating and the Pt nanoparticles.

Fig. 4 illustrates the SIMS profiles as a function of erosion time, of Al^+ , of CsAl^+ (complex ion composed of a Cs^+ ion from the SIMS ion beam, stuck to an Al atom and preferentially related to metallic Al), of CsO^+ and of CsTi^+ (preferentially related to metallic Ti), in the oxidized sample Cod2. Similar profiles are obtained from sample Cod1. It can be noticed that profiles of Al^+ and of CsO^+ are similar, indicating that oxygen is preferably linked with Al. Ionic Al is found at the external part of the coating and it decreases with erosion time. An increase of the concentration of metallic Al (CsAl^+) is found at intermediate depth corresponding to the previously mentioned interdiffusion zone. The concentrations of both metallic and ionic Ti are very low in the coating. Although the present analysis was not optimized for elements quantification, it is worth noting that the relative intensities of CsAl^+ and CsTi^+ in the interdiffusion zone roughly correspond to Al/Ti ratio of 3, which is compatible with the Al_3Ti compound identified by XRD. An increase of ionic Ti before the interdiffusion zone indicates localized oxidation of Ti at that position. Finally, Pt concentration is limited in the coating by the interdiffusion zone, confirming the low diffusion rate of Pt in Ti, compared with that of Al.

The main developed scales at the surface of the Cod2 coating are $\delta\text{-Al}_2\text{O}_3$ (JCPDS #160394) and $\gamma\text{-Al}_2\text{O}_3$ (JCPDS #100425). It was not possible to unambiguously identify titanium oxides, confirming the efficiency of the deposited protective coating.

Many of the characteristics of the presented morphology and microstructure of the Cod2 coating are found in the other samples as well. For example, in all oxidized samples Pt is systematically located at the interface with the substrate. This is possibly due to the very fast diffusion of the Al from the coating to the substrate with subsequent “filtering” (concentration) of the Pt at the Ti6242–Al interface.

Morphology of samples Seq1, Cod1 and Cod2 is systematically more compact and smooth than that of sample Seq0 (mean roughness $R_a=1.5\ \mu\text{m}$ for Seq0 and

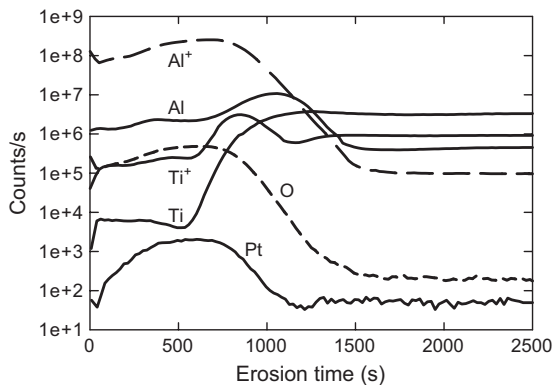


Fig. 4. SIMS element profiles as a function of erosion time for sample Cod2.

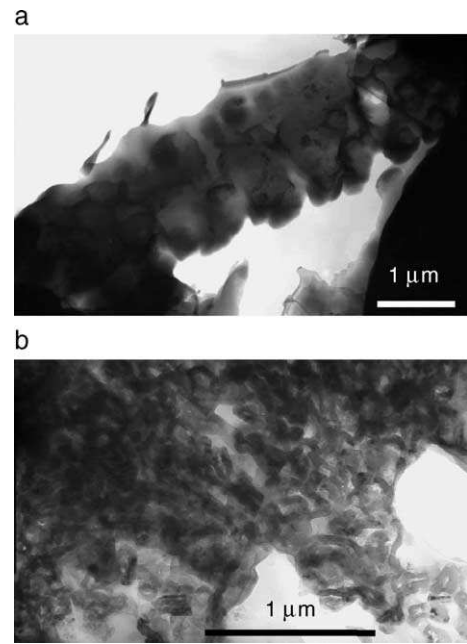


Fig. 5. Bright field TEM micrographs of the alumina scale of sample Cod2 (a) and Seq2 (b).

$R_a=0.5\ \mu\text{m}$ for Cod2). Due to its loose morphology Seq0 does not act as diffusion barrier against Ti migration to the surface, allowing the formation of titanium oxide in the coating as was revealed by SIMS and XRD in this particular case.

Fig. 5 presents two TEM cross sectional micrographs of the Al_2O_3 scale of sample Cod2 (a) and of a non-optimized sequential coating processed in conditions Seq1 (b). In the former case, the Al_2O_3 layer is compact, well crystallized with no porosity. In contrast, the Al_2O_3 in the later case presents an extended open porosity. Even if preparation of cross sections may be partially responsible for the extension of this microstructure, the fact that both samples were prepared following the same protocol allows one to conclude that a more compact morphology of the Al_2O_3 layer is formed on Cod2 resulting in increased protection against oxygen ingress towards the alloy.

4. Conclusions

Oxidation kinetics and microstructure of Al–Pt coatings on Ti6242 alloy were investigated. These coatings were processed by MOCVD from $\text{Me}_3(\text{MeCp})\text{Pt}(\text{VI})$ and DMEAA and were subjected to isothermal oxidation in a thermobalance at 873 K for 90 h under synthetic air flow. Three coating architectures were investigated, namely for pure Al, Pt and Al sequential sublayers, and co-deposited Al and Pt. Oxidation kinetics systematically revealed a strong transient oxidation regime followed by a diffusion driven parabolic kinetics. Optimized sequentially deposited and codeposited coatings revealed a noticeable protection against oxidation, with more than one order of magnitude

lower oxidation kinetics than that of the bare alloy. The performance of the plain Al is non-negligible, suggesting that a direct platinum effect does not apply to isothermal oxidation behavior for coatings manufactured by MOCVD onto titanium alloys. The latter is rather depending on the surface morphology and the coating microstructure. The loose, porous microstructure of the plain Al coating can be improved by an appropriate selection of the Al precursor and by driving the surface chemistry through the use of surfactants such as C_2H_5I and of H_2 in the reactive gas phase. Such improved coatings yield oxide scales composed of compact $\delta-Al_2O_3$ and $\gamma-Al_2O_3$.

The MOCVD processed Pt-modified Al coatings on Ti6242 show satisfactory performance under isothermal oxidation tests. However, they could be further improved to reduce both transient and steady state oxidation kinetics by optimizing surface chemistry and by controlling coatings microstructure more accurately. Cyclic oxidation tests are in progress to approach extreme operating conditions of helicopter turboengines and they may reveal the role of the composition of the coatings, namely the presence of Pt, in modifying the performance of the coating against oxidation.

Acknowledgements

We are indebted to Claude Armand of the SIMS facility at the Institut National de Sciences Appliquées of Toulouse for samples characterization. This work is part of the APROSUTIS project supported by the Réseau National Matériaux et Procédés (RNMP) network. It was performed through a grant accorded to MD by the French Ministry of Education.

References

- [1] J.R. Nicholls, MRS Bull. 28 (2003) 659.
- [2] M. Delmas, M. Ucar, L. Ressler, M. Pons, C. Vahlas, Surf. Coat. Technol. 188–189C (2004) 49.
- [3] T.W. Jang, W. Moon, J.T. Baek, B.T. Ahn, Thin Solid Films 333 (1998) 137.
- [4] Y. Neo, M. Niwano, H. Mimura, K. Yokoo, Appl. Surf. Sci. 142 (1999) 443.
- [5] D. Monceau, B. Pieraggi, Oxid. Met. 50 (1998) 477.
- [6] I. Gurrappa, A.K. Gogia, Surf. Coat. Technol. 139 (2001) 216.
- [7] A.L. Purvis, B.M. Warnes, Surf. Coat. Technol. 146–147 (2001) 1.